Optical Communications for High-Altitude Platforms

Franz Fidler, Markus Knapek, Joachim Horwath, and Walter R. Leeb

(Invited Paper)

***Abstract*—This paper contains a review of technologies, theoretical studies, and experimental field trials for optical communications from and to high-altitude platforms (HAPs). We discuss the pointing, acquisition, and tracking of laser terminals and describe how laser beams with low divergence can be used to transmit data at multi-Gigabits per second. Investigating the influence of the atmosphere, background light, and flight qualification requirements on system design, we explain why the data rates in free-space optical communications are still significantly below those possible in today's terrestrial fiber-based systems. Techniques like forward-error correction, adaptive optics, and diversity reception are discussed. Such measures help to increase the data rate or link distance while keeping the bit error ratio and outage probability of the optical HAP communication system low.**

***Index Terms*—Free-space optical (FSO) communication, high-altitude platform (HAP), laser beams, optical components, system analysis and design, terrestrial atmosphere.**

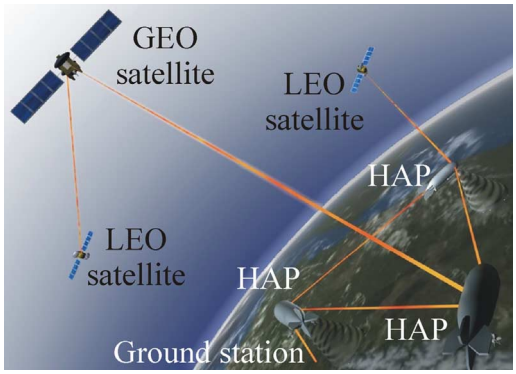

Fig. 1. Laser communication scenarios from HAPs.

I. Introduction

FREE-SPACE laser communications uses collimated laser beams to transmit information at high data rates in the multigigabit regime, preventing interference problems and exhaustion of radio-frequency (RF) bandwidths. Using lightweight and compact terminals, optical intersatellite links and orbit-to-ground links are already operable [1]–[3], the latter suffering from cloud coverage [4], harsh weather conditions, and atmospheric turbulence [5]. Current research also investigates optical communications from or to high-altitude platforms (HAPs) [6], [7]. HAPs are aircraft or airships situated well above the clouds at typical heights of 17 to 25 km, where the atmospheric impact on a laser beam is less severe than directly above ground [5]. As depicted in Fig. 1, optical links between HAPs, satellites, and ground stations are envisioned to serve as broadband backhaul communication channels if data from various sensors or RF communication terminals onboard the HAP is to be transmitted, or if an HAP works as a data relay station. In Sections II and III, we discuss some key concepts and technological requirements of the optical communication system, where the difficulty of in-line amplification between transmitter and receiver requires highly sensitive receivers and appropriate modulation formats. As outlined in Section IV, a pointing, acquisition, and tracking (PAT) system has the task of setting up and tracking the link, which is often difficult to achieve due to the small divergence angle of the laser beam [8]. Because the laser light has to travel through the atmosphere [9], we investigate atmospheric channel models in Section V, which are applicable to communications links from and to HAPs. The models allow to quantitatively estimate the impairments due to atmospheric turbulence, such as additional beam spreading or wavefront distortions. Accurate modeling will allow for the design of appropriate mitigation measures, like adaptive optics (AO), diversity reception, or forward-error correction (FEC) with the aim to reduce the bit-error ratio (BER) of the communication link. System performance is also influenced by the quality of the transmit signal or, as outlined in Section VI, by additional noise sources, such as background light from celestial bodies. Section VII then gives an overview on a number of theoretical and experimental system studies that have been conducted for optical satellite-to-HAP, HAP-to-HAP, as well as ground station-to-HAP communication and networking scenarios.

HAPs are quasi-stationary vehicles like helium-filled airships that operate in the stratosphere well above civil air routes, jet-streams, and clouds, but substantially below orbiting satellites [10]. Remote-operated or autocontrolled lightweight planes at such altitudes, which need to fly against the wind or in a circular path, are generally referred to as unmanned aerial vehicles (UAVs). HAPs and UAVs provide a platform for scientific, military, or commercial payloads. UAVs need to be in motion to generate lift, and thus, the payload capacities are limited to 50–300 kg [6], [11]. HAPs are expected to support payloads up to 2000 kg. Another difference is the available power. Current estimates are up to 3 kW at UAVs and 10–15 kW at HAPs. Table I

Manuscript received October 12, 2009; revised January 16, 2010; accepted March 26, 2010. Date of publication May 17, 2010; date of current version October 6, 2010. This work was supported by COST297 (European Cooperation in Science and Technology: High-Altitude Platforms for Communications and Other Services) under the Sixth European Research and Technological Development Framework Program.

F. Fidler and W. R. Leeb are with the Institute of Communications and Radio-Frequency Engineering, Vienna University of Technology, Vienna A-1040, Austria (e-mail: ffidler@nt.tuwien.ac.at).

M. Knapek and J. Horwath are with the Institute of Communications and Navigation, German Aerospace Center (DLR), Wessling 82234, Germany (e-mail: markus.knapek@dlr.de).

Color versions of one or more of the figures in this paper are available online at http://ieeexplore.ieee.org.

Digital Object Identifier 10.1109/JSTQE.2010.2047382

TABLE I
EXAMPLES OF HAPS

Name	Country	Manufacturer	Altitude
HAA	USA	Lockheed Martin	20 km
HALE	EU	Lindstrand Balloons	20 km
X-Station	CH	StratXX Holding AG	21 km
Global Hawk / Euro Hawk	USA / DE	Northrop Grumman / EADS	20 km
Global Observer	USA	AeroVironment	20 km
Zephyr / Mercator	UK	QinetiQ	18 km

lists example of high-altitude aircrafts and airships, which, in part, are still under development.

Combining the features of terrestrial and satellite communication, HAP-based systems offer a number of benefits, like a reduced shadowing from terrain, a wide service coverage area of 200–500 km diameter, rapid deployment, easier servicing and lower cost than with satellites, environmental advantages by reducing the need of terrestrial infrastructure or rocket launches, no requirement for space-qualified components (but still some flight qualification), and less atmospheric influence than for ground stations.

The applications of HAPs have been the subject of considerable interest and activity internationally for the past few years [6]. There are several ongoing and finished projects worldwide, including programs in the USA (e.g., Helios), Europe (e.g., CAPANINA, HAPCOS, HeliNet, SatNEX), and Asia (e.g., SkyNet) often involving national space agencies like National Aeronautics and Space Administration (NASA), European Space Agency (ESA), Japan Aerospace Exploration Agency (JAXA), German Aerospace Center (DLR), or Korea Aerospace Research Institute (KARI).

1) HAPs may be used as platforms for remote sensing, i.e., data about an object are collected via various sensors without getting into direct contact with the object itself. Applications are geographical mapping, astronomical observations, military tasks, surveillance of big events, traffic, country boarders, or disasters, collection of meteorological data, as well as scientific remote sensing to monitor environmental media, like air, land, or water.
2) Using HAPs can be of great importance in scarcely populated areas with little or no infrastructure. In the event of a disaster, broadcasting or telecommunication from HAPs can be used for wireless "last-mile" access.
3) In quantum cryptography, HAPs could accommodate entangled photon sources to distribute a secure key to users on the ground, to other HAPs, or to a satellite.
4) Because of the large coverage area, HAPs could play an active role in navigation and localization to accurately detect the position of a target on the ground or in the air.

In all these scenarios, the platform may be required to send a large amount of data from a number of sensors or users to a ground station or to a satellite via a high-data-rate link. In such a case, laser-based free-space communication systems are attractive contenders and, as discussed in Section VII, have been the topic of a number of experimental and theoretical studies, field trials, and measurement campaigns. While RF links are typically limited to a few 100 Mb/s [12], [13], free-space optical (FSO) communication links offer much larger data rates. Optical HAP-to-ground communication trials have already been achieved up to 1.25 Gb/s [14]. Theoretical studies were conducted showing the potential for data rates up to 10 Gb/s to be sent from and to HAPs [15].

II. FSO COMMUNICATIONS

The diffraction-limited beam divergence of a laser beam is determined by its wavelength λ, the transmit telescope diameter D_T, and a divergence factor d_f accounting for beam truncation and obscuration by the telescope assembly [16]

$$\theta = d_f \frac{\lambda}{D_T}. \tag{1}$$

Due to the small wavelength, the beam is very narrow, which allows interference-free and secure operation and leads to a high antenna gain even with small telescope diameters. Typical optical antenna diameters—below 30 cm—in general lead to a reduced flight-terminal mass and small momentum disturbances compared to RF communication systems [13].

A. Link Budget

Link-budget calculations estimate the received optical power P_R for a link with power P_T available at the transmitter, a link distance L, a gain G_T of the transmit antenna, and the effective area A_R of the telescope serving as receive antenna. As indicated in (2), implementation losses within the transmitter and the receiver η_T and η_R, respectively, pointing losses a_P (see cf., Section IV), and losses caused by the atmosphere a_A (see cf., Section V) may reduce the received power P_R considerably (η_T, η_R, a_P, and a_A, all <1), thus leading to

$$P_R = P_T \frac{G_T A_R}{4\pi L^2} \eta_T \eta_R a_P a_A. \tag{2}$$

The far-field on-axis antenna gain G_T is related to the effective area of the transmit telescope A_T as follows [16]:

$$G_T = \frac{4\pi A_T}{\lambda^2} g_T \tag{3}$$

with $g_T = 1$ in the ideal case. In practice, the emitted beam often resembles a truncated Gaussian distribution, partially obscured by a secondary mirror and antenna struts, and with some wavefront distortions caused by imperfect optics. Hence, the gain may be reduced by a factor of some $g_T \approx 0.6$, but still (for typical λ and D_T) amounts to approximately 110 dB.

B. Terminal Design

Terminals for optical communications are mostly designed for bidirectional links. They comprise both a transmitter and a receiver that generally share the optical antenna. Another peculiarity is the necessity of beam steering with submicroradian angular resolution. These requirements lead to a transceiver block diagram, as shown in Fig. 2.

To achieve the highest possible antenna gain, the laser source preferably operates in a single transverse mode. For signal transmission, the modulated beam passes an optical duplexer and a fine-pointing assembly before it enters a telescope acting as

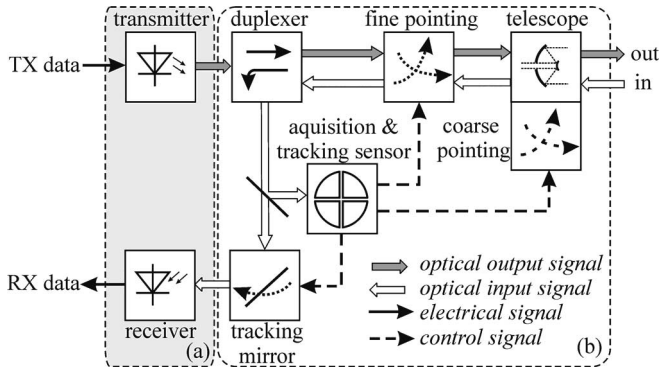

Fig. 2. Laser communication terminal structure. (a) Communication subsystem. (b) PAT system.

transmit antenna. A coarse-pointing system provides for antenna steering. In a two-way link, the duplexer assures sufficient isolation between the powerful transmit signal (on the order of 30 dBm) and the weak receive signal (on the order of −40 dBm) through the use of orthogonal polarizations and/or the use of different wavelengths.

The received radiation passes the antenna and the fine-pointing assembly in reverse direction, and is then directed to the receive part of the terminal. Another section is used for controlling the fine- and coarse-pointing mechanisms in such a way that the acquisition and tracking detector is always hit centrally. For scenarios with an appreciable transverse movement of the two terminals, a point-ahead mechanism has to be inserted in either the receive or the transmit path to take into account the slightly different direction of incoming and outgoing beam. If there is a relative movement between the two terminals to be linked, the received signal will be Doppler-shifted. This effect may amount to several gigahertz [17] and might require a wide-frequency tuning range of optical input filters or of local oscillator lasers in coherent optical links.

C. Telescopes

For optical antennas, reflective systems using lightweight mirrors are preferred over refractive structures. Requirements like the maximum allowed size and mass, the minimum antenna gain, the required field-of-view (FOV), the maximally allowed laser beam obscuration and truncation, as well as alignment tolerances, and the thermal environment determine the design parameters of the optical antenna. A number of different concepts have been studied for FSO communications [12]. The Cassegrain reflector is a combination of a primary concave mirror and a secondary convex mirror. In a symmetrical design, both mirrors are aligned along the optical axis, with the primary mirror usually containing a hole in the center, thus permitting the light to reach the transceiver assembly. Such center-feed telescopes are already employed successfully on optical communication satellites like Advanced Relay and TEchnology MIssion Satellite (ARTEMIS) (optical payload for inter-satellite link experiment (OPALE) terminal) [18], Satellite Pour l'Observation de la Terre (SPOT)-4 (PASTEL terminal) [18], or Optical Inter-Orbit Communications Engineering Test Satellite (OICETS) (laser-utilizing communications equipment (LUCE) terminal) [2]. As a demonstration terminal for airborne platforms, *RUAG Space AG* designed the nondiffraction-limited OPTEL-AP [19] to produce a complete Ritchey–Cretien–Cassegrain-type telescope of 25 cm diameter. The telescope has a weight of 22 kg and its pointing system consumes 15 W of electrical power. A Schiefspiegler is another variant of the Cassegrain design with off-axis mirrors to avoid the secondary obscuration [14], [20].

III. Optical Communications Subsystem

The optical communication subsystem deals with all aspects of the information transport itself. The selection of an appropriate modulation format, a transmitter with large optical output power, as well as a highly sensitive receiver setup is important to achieve a satisfactory performance. Quantitative measures for the performance are, for example, the achievable BER, the available power margin, and the system outage probability.

A. Receiver

The receiver converts data carried by the optical input signal into an electrical output signal. Because of no in-line amplification between transmitter and receiver, a high receiver sensitivity is required. This sensitivity is expressed by the number of photons per bit or by the optical power at a given data rate required to achieve a certain target BER.

Two basically different receiver concepts may be distinguished: coherent and direct detection (DD). The *coherent* scheme uses a local laser oscillator (LO) to increase the photodetector output signal. At the photodiode, the LO signal beats with the communication signal, thus yielding a photocurrent term proportional to the optical field strength [21]. This scheme features high sensitivity and low susceptibility to background radiation. In homodyning, the optical signal is directly transferred into the baseband, while in heterodyning and intradyning, there is a frequency difference between the LO and the signal, thus resulting in an IF in the RF regime. Coherent detection places strict requirements on the spectral purity of the lasers. It demands that the received signal and the local oscillator should have spatial phase fronts nearly aligned perfectly over the active area of the detector. The most important requirements for LO lasers are transverse and longitudinal single-mode operations so that the IF is centered at a single carrier, narrow linewidth to minimize laser phase noise, and frequency tuneability to compensate for variations in transmit laser frequency and for Doppler shift. Recent progress in high-speed digital signal processing (DSP) also enables the use of a free-running LO [22]. The signal is digitized after reception and a DSP corrects for frequency and phase offsets between transmission laser and LO. Coherent detection was successfully implemented for the intersatellite link between the German satellite TerraSAR-X and the US satellite near field infrared experiment (NFIRE) [3], but is still used to a much lesser extent than DD receivers [1], [2], [12], [14].

In a DD receiver, the photodiode current is proportional to the power of the received signal. Hence, any phase or polarization information is lost, thus restricting the modulation format to intensity modulation if no additional preprocessing is used. DD offers advantages over coherent detection in terms of cost and complexity, when the temporal coherence of the transmit laser

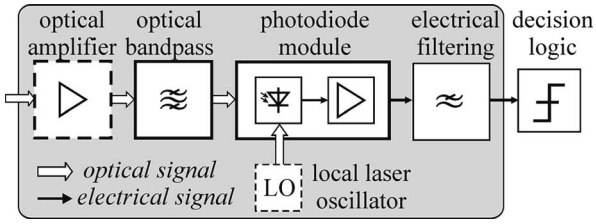

Fig. 3. Generic block diagram of a digital optical receiver.

TABLE II
TYPICAL PARAMETERS OF PHOTODIODES FOR FSO COMMUNICATION SYSTEMS AT DATA RATES UP TO 10 Gb/s

	PIN		APD	
	Si	InGaAs	Si	InGaAs
Wavelength range [μm]	0.5-1.1	1-1.6	0.4-1.06	0.9-1.6
Primary sensitivity [A/W]	0.7 at 950 nm	0.9 at 1550 nm	0.65 at 950 nm	0.8 at 1550 nm
Total dark current [nA] at room temperature	1	1	3	100
Bias voltage [V]	-5	-5	160	35
Multiplication factor M	1	1	100	10

or the LO cannot be sufficiently controlled, or when the spatial phase characteristics of the received wave is disturbed.

Fig. 3 shows a schematic of a receiver, which in its simplest form, comes without the dashed subunits. Optical preamplification is optional, while an optical bandpass filter centered at the carrier wavelength is usually implemented to reduce background radiation (and possibly amplified spontaneous emission (ASE) noise from a preamplifier). After passing the filter, the data signal is converted into an electrical current using a photodetector. Baseband processing is followed by sampling and decision.

The *photodetector* is usually implemented either as a p-i-n-photodiode or an APD. One of its main characteristics, besides the response time, is the responsivity S. It is defined as the current-to-optical-power ratio (in amperes/watt). Its maximum values are typically around 0.7 A/W at 950 nm for Si-devices and 1.1 A/W at 1550 nm for InGaAs [12]. An APD multiplies the generated primary photoelectrons by its avalanche gain M (e.g., $M \approx 100$ for Si APDs and $M \approx 10$ for InGaAs APDs). This effect comes at the expense of multiplication noise. Table II presents typical parameters for 10 Gb/s devices.

Where APDs cannot provide enough bandwidth, low-noise *optical preamplification* may improve the sensitivity of optical receivers considerably, approaching the quantum limit within a few decibels [15]. To date, mainly Erbium-doped fiber amplifiers (EDFAs) have been employed in FSO high-data-rate receivers. These EDFAs are engineered for single-transverse-mode operation, which means that the received radiation is required to be coupled into a single-mode fiber. EDFAs, available for both the C-band (1530–1560 nm) and the L-band (1570–1600 nm), operate close to the theoretical 3 dB noise figure, and gains of $G > 35$ dB are easily achieved [12].

B. Modulation Formats

To transmit information over an optical channel, several ways exist to imprint data onto the laser beam. We can modulate the amplitude, the phase (frequency), or the polarization of the optical signal. While there is a large number of advanced optical modulation formats, which are considered suitable for fiber-based communication [23], only a few modulation formats have been studied so far with respect to FSO communications from HAPs—mainly intensity-modulated OOK [14], [15], [24], BPSK [25], differential phase-shift keying (DPSK) [17], [26], and polarization shift keying (POLSK) [27].

TABLE III
SENSITIVITY OF MODULATION AND DETECTION TECHNIQUES STUDIED FOR HAP APPLICATIONS

	Detection technique	QL [ppb]	Sens [ppb]	BER	R [Gb/s]	Ref.
OOK	DD, preamp.	41	70	10E-9	10	[15] Sim
			73	10E-9	1	[15] Sim
	DD, APD	20	140	10E-6	1.25	[25] Exp
			1565	10E-9	2.5	[29] Sim
	-	-	3122	-	2.5	[30] Exp
DPSK	DD, preamp.	20	39	10E-9	10	[31] Sim
			56	-	10	[17] Sim
BPSK	coherent	9	40	10E-6	1	[25] Exp
POLSK	DD, preamp.	40	74	10E-9	10	[27] Sim

DD: direct detection, preamp: optical preamplification, APD: avalanche photodiode, QL: quantum limit, ppb: photons per bit, sens: sensitivity, BER: bit error ratio, R: data rate , Sim: simulation, and Exp: experiment.

While [12], [23], and [28] give a good overview on sensitivity records already achieved with these modulation formats, Table III concentrates on calculated and measured sensitivities specifically from studies on optical communications for HAPs. OOK DD systems in combination with optically preamplified receivers usually show a sensitivity around 70 to 80 photons/bit (ppb) at a BER $= 10^{-9}$. With APD-based receivers, the sensitivity typically stays well above 140 ppb. While DPSK offers a 3 dB gain compared to OOK [23], a 3.2 dB advantage of POLSK over OOK can only be achieved in peak-power-limited systems and when using balanced detection [27]. A typical value for the sensitivity of existing coherent systems when using BPSK modulation is 40 ppb for a BER $= 10^{-6}$ [25].

Not every reception technique is suited for each modulation format. DD receivers are insensitive to phase and polarization information and require conversion into OOK by means of external optical components, e.g., with delay demodulators for DPSK [23] or polarization filters for POLSK [27]. Coherent receivers detect the optical field directly, thus allowing for any modulation format without optical preprocessing.

C. Transmitter

The transmitter generates laser light to imprint data onto the optical carrier and to amplify the optical output power. The block diagram of a basic transmitter setup is shown in Fig. 4. A continuous wave or directly modulated laser module serves

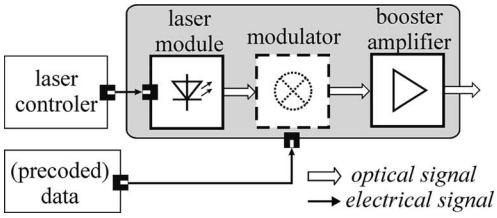

Fig. 4. Generic block diagram of digital optical transmitter.

as a source and determines the operation wavelength of the system. Mach–Zehnder modulators (MZMs) or electroabsorption modulators (EAMs) can be used in order to establish advanced modulation schemes and to achieve sufficiently high extinction ratios. Phase modulation can be achieved either via an MZM or a dedicated phase modulator [23]. Various designs of polarization modulators have also been proposed, mostly based on $LiNbO_3$ devices to allow for high data rates.

If the wavelength of the laser is set within the C-band (from 1530 to 1560 nm), the modulated data signal can be amplified by a booster EDFA to achieve an optical output power of up to 10 W before it is fed to the transmit telescope assembly [15]. Coherent systems have highly rigorous phase-noise requirements and are therefore mainly the domain of solid-state lasers, e.g., Nd:YAG at 1064 nm [3]. Even at this wavelength, optical amplifiers have been implemented, based on Yb-doped fibers and with output powers up to 8.8 W [32]. In general, the selection of the transmitter's wavelength is not only driven by the receiver concept, but also by the desire to minimize atmospheric attenuation, the required quality of the optics, the required output power, the flight qualification requirements, and cost.

D. Flight Qualification of Components

Optical terminal hardware for the stratospheric environment has to meet higher environmental specification requirements than commercial off-the-shelf telecommunication equipment. Using space-qualified components would be straightforward, but aside from their prohibitive cost and poor availability, space-qualified versions of industrial components rarely represent state-of-the-art micro- and optoelectronics. To start the development based on military (MIL) standard specified components and subassemblies is a feasible approach. Except for radiation tolerance and operation in vacuum, MIL-standard-qualified components meet nearly all of the demanding requirements of airborne operations [12].

1) Thermal Constraints: The low ambient temperatures down to $-70\,^{\circ}\mathrm{C}$ are a challenge for the highly precise mechanical pointing elements. Large temperature gradients between terminal functional blocks that act as heat sources, e.g., pump lasers, processors, or terminal parts exposed to solar radiation, and cold terminal parts, like the coarse-pointing assembly and telescope, can cause additional problems. The preferred design approach is to advantageously use convection to prevent stress and loss of adjustment of optical components and to create favorable temperature equilibria within the terminal.

2) Vacuum Constraints: The pressure during the nominal HAP station-keeping maneuver depends on the altitude and is between 5 and 50 mbar. Compared to 1 bar, the efficiency of convective heat transfer is virtually not existent. Thus, radiative heat transfer is the only effective way for power dissipation. Heat pipes inside the optical terminal feeding heat radiators at the surface are installed for that purpose. Vacuum-tight subassemblies filled with atmosphere (and hence water vapor) and containing optical elements pose a special problem. Because environmental temperatures on HAPs may be as low as $-70\,^{\circ}\mathrm{C}$, ice crystals could adsorb on optical surfaces. This problem can be prevented by using, e.g., N_2 gas during integration. Otherwise, enclosed volumes have to be avoided by incorporating vents into the design.

3) Radiation Constraints: For all the devices constituting the optical communication part of the terminal, sensitivity to hard radiation is an issue mainly for the optical amplifiers with Erbium-doped fiber (EDF). To optimize EDF for active applications, dopants such as Al and La are added to the glass composition. These dopants are likely to substantially increase the fiber radiation sensitivity and the fiber is prone to darken [12]. In the stratosphere, the atmosphere absorbs a great part of cosmic rays and radiation. In this regard, qualification of components is less strict for HAPs than for outer-space systems [33]. However, depending on solar activity, the increased radiation at such altitudes can lead to malfunctions in digital hardware during program code executions, e.g., to a change of the register content, within CPUs and DSPs.

4) Vibration Requirements: Vibration strengths depend on the type of HAP (aerostatic or aerodynamic) and on the propulsion system. Fiber-based concepts, where connectors are used instead of multiple optical elements for beam guidance, help to reduce vibration sensitivity.

5) Payload Limitations: As discussed in Section I, the weight and power consumption of the payload is limited depending on the platform. Table IV gives examples for existing terminals.

TABLE IV
MASS AND POWER CONSUMPTION OF OPTICAL COMMUNICATION TERMINALS

	Terminal	Weight [kg]	Power consum. [W]	Ref.
Satellite (Artemis)	OPALE	160	150	[34]
Satellite (SPOT-4)	PASTEL	150	150	[34]
Satellite (OICETS)	LUCE	140	230	[35]
Satellite (TerraSAR-X)	LCT	< 50	150	[20]
HAP (STROPEX)	FELT	18	75	[14]
HAP	Optel-AP	~ 50	< 165	[19]

IV. POINTING, ACQUISITION, AND TRACKING

While the use of short wavelengths provides high antenna gain, the resulting narrow beams lead to pointing and tracking challenges. In order to successfully establish an optical free-space link, PAT systems operate in three phases [8].

Pointing is done by directing the outgoing beam toward the receiver, based on (often GPS-assisted) *a priori* knowledge of the transmitter and receiver positions. Pointing is performed either by moving the whole telescope with a two-axis gimbal [36] or via a coarse-pointing mirror.

Acquisition is the process when the exact positions of the transmitter and receiver are detected and the laser beams are readjusted accordingly. A common technique is to place a beacon laser at the transmitting platform and point it toward the receiver [8], [14]. To generate a beacon beam with a larger divergence angle, lasers operating at wavelengths differing from that of the communication laser can be used. The PAT system has to find this beacon, which is usually done by moving the beacon beam within an uncertainty area, while the other terminal also scans the uncertainty region using a detector with a narrow FOV. After each terminal has detected a beacon of the respective other terminal, the communication lasers are switched ON and the tracking phase begins.

Tracking assures that the transmit laser is kept targeted onto the receiver. First, coarse tracking is performed by means of a control loop driving a coarse-pointing mirror. Then, a tracking loop controls the fine steering mirror, which should have a bandwidth of $\geq$1 kHz to accommodate vibrations. The angular error between the direction of the incoming and outgoing beams serves as a feedback for the tracking mirrors. Charge-coupled device (CCD) arrays, CMOS-arrays (active pixel sensors), or quadrant (avalanche) photodiodes (QPDs) can be employed as tracking sensors. Often CCDs are used for coarse tracking and QPDs for fine tracking because the former offer a wider FOV, while the latter are faster and more accurate. Tracking errors can have a high impact on the link attenuation and should be considered in the link-budget calculations. To compensate for the pointing error caused by the finite speed of light and the normal component of the relative velocity between terminals, a point-ahead angle is applied. The transmit beam is directed to the location where the receiver will be situated after propagation time [8].

When designing PAT systems for HAPs, a number of peculiarities have to be taken into account, which are as follows.

1) The wavelength of the beacon laser has to be chosen in accordance with the wavelength-dependent atmospheric attenuation. Beacon wavelengths traditionally used in FSO systems are 800–850 nm [2], [30] or 980 nm [14], [30].
2) Vibrations and rotation frequencies can be much higher than on a satellite. In [14], a spin rate of 9 rotations per minute was reported, which led to the design of a PAT system with a maximum rotation speed of 240°/s. The elevation axis of this telescope assembly can be moved at 120°/s. For more stable platforms, angular dynamics of 10°/s could be sufficient [19].
3) Robust acquisition has to be guaranteed in the presence of strong background light also, e.g., due to scattering from Earth or the atmosphere.
4) Airborne platforms usually have a much lower accuracy in attitude determination than satellites. This has to be taken into account for the initial acquisition process. For example, the HAP has to be first illuminated by the ground station beacon before the flight terminal can acquire the link within its relatively large uncertainty cone of a few degrees [14].

V. Atmospheric Impact

The Earth's atmosphere extends approximately 700 km above the surface and consists of several distinct layers [5]. Pronounced density is found within the lowest 20 km, still influencing HAP communication links. When a laser beam propagates through a turbulent medium, like the atmosphere, one observes absorption, scattering, additional beam spreading and beam wander, scintillation, and phase-front distortions. These phenomena result in loss of power; the latter three in intensity fluctuations, i.e., fading, at the receiver. Fading may lead to link failures during certain periods of time. While some measured data and mathematical models are available in the literature for ground–satellite links [5], [37], such information is scarce for optical links from or to HAPs. In the following section, we discuss a number of degrading effects and present methods for their quantitative estimation.

A. Absorption and Scattering

Absorption exhibits a strong dependence on wavelength [37]. In practice, only atmospheric windows, where the attenuation is minimal, are suitable for FSO. The typical laser communication wavelengths 1.064 and 1.55 μm, as well as the interval between 10 and 12 μm fall into good transmission windows [4], [37]. Atmospheric scattering due to molecular-sized particles is called Rayleigh scattering. It is dominant for clear sky conditions and is proportional to λ^{-4}. For large particles compared to the wavelength, Mie scattering occurs, which does not have a strong dependence on λ.

When transmitting an optical signal along a vertical path from the ground through the atmosphere, some 1 to 2 dB of atmospheric loss a_A have to be expected for clear skies, at zenith, and at $\lambda = 1550$ nm due to absorption and scattering [37]. If the transmitter is situated at HAP at 20 km height, this value reduces to 0.2 dB [38]. The variation of the atmospheric attenuation with zenith angle ζ, which is the angle between zenith and the line-of-sight (LOS) between transmit and receive telescope, can be approximated as follows [31]:

$$a_A(\zeta) = a_A(0)\sec(\zeta) \quad \forall\, 0 \leq \zeta < 70^\circ. \tag{4}$$

The resulting loss of 0.2 to 0.8 dB for typical HAP-satellite links is not a dominant part in the link budget.

The situation is different for horizontal HAP-to-HAP links.

In long atmospheric paths, the aerosol condition has to be taken into account, which is dominated by the grade of volcanic activity. In the case of a volcanic eruption, aerosols penetrate the stratosphere and are distributed over the whole globe within a few weeks, thus leading to increased aerosol absorption during an extended period of time. However, such events are rare, and thus, should not limit the applicability of HAP-to-HAP optical links. Fig. 5 gives an example of the extinction coefficient α with and without volcanic activity for a 780 km link between two HAPs at 25 km altitude and at a wavelength of $\lambda =$ 800 nm [39]. Moving along the link path from the transmitter to the receiver, the extinction coefficient shows two peaks in the case of volcanic activity, at a link altitude of 20 km where the aerosol density is maximal [38]. The minimum in between is at a link altitude of 13 km. At 800 nm, Rayleigh scattering is still relatively strong. For a wavelength of 1064 nm, the two peaks would just reach 0.008 and 0.004 km^{-1} for 1550 nm. Because α reduces the transmitted optical power along the path z

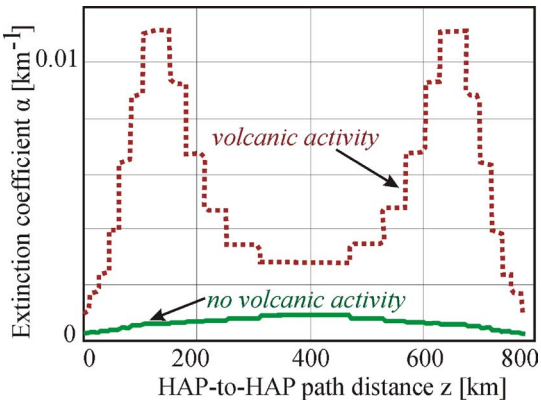

Fig. 5. Extinction coefficient α due to absorption and scattering versus HAP-to-HAP path distance [39].

according to

$$\exp\left(-\int_0^L \alpha\left(z,\lambda\right)dz\right) \tag{5}$$

the minimal and maximal attenuation at large zenith angles ($>70°$) range between 2.2 and 18.3 dB for 800 nm, between 0.89 and 12.3 dB for 1064 nm, and between 0.26 and 6.27 dB for 1550 nm.

B. Beam Spread

Atmospheric turbulence causes beam spread beyond the diffraction-limited divergence [40], θ_{DL}, thus leading to an effective divergence angle [5] θ_{eff}, thus resulting in a reduction of the mean received optical power by a factor $(\theta_{\mathrm{eff}}/\theta_{\mathrm{DL}})^2$. If any turbulence is weak and relatively far away from the transmitting source, e.g., in satellite-to-HAP downlinks, the effective spot size at the receiver is essentially the same as the diffractive spot size. Hence, beam-spread loss is negligible. In the uplink, where the size of turbulent eddies, situated just in front of the transmitter, is large relative to the beam diameter, the mean beam-spread loss may range, e.g., from 3 dB in a ground-to-satellite scenario to 0.03 dB in an HAP-to-satellite uplink [15].

C. Fading

Variations of the received signal intensity due to interferometric effects and beam wander are usually called *fading*. Turbulent motion of the atmosphere in the presence of temperature and pressure gradients causes disturbances in the atmosphere's refractive index in the form of eddies, acting as random optical lenses that refract the propagating light. One may distinguish between the following two main effects.

1) Deflections along the propagation path move the beam profile randomly off the LOS between transmitter and receiver. The instantaneous center of the beam, i.e., the point of maximum intensity, is randomly displaced in the receiver plane. This *beam wander* is caused mainly by large-scale turbulence near the transmitter, and thus, can typically be neglected for satellite-to-HAP downlinks [5].
2) *Scintillation* is caused by random index-of-refraction fluctuations. It leads to both the temporal variation in received power and the spatial variation within a receiver aperture. Its quantitative measure is the *scintillation index* σ_I^2, i.e., the variance of intensity fluctuations normalized to the square of the mean intensity

$$\sigma_I^2 = \frac{\langle I^2\rangle}{\langle I\rangle^2} - 1 \tag{6}$$

where $\langle I\rangle$ is the temporal mean intensity of the optical wave at the receiver [37]. Such $\sigma_I^2 \leq 1$ corresponds to weak fluctuations, whereas $\sigma_I^2 > 1$ is referred to as moderate-to-strong fluctuation regime. Simulations using the analytical formulas, as given in [5], [31], show that—contrary to satellite–ground links—the scintillation parameter is typically between 0.3 and 0.8 for HAP-to-HAP scenarios [41], between 0.28 and 1.12 for HAP–ground scenarios [9], and ranges down to values below 0.025 for HAP-satellite links [15].

Fading leads to a certain dynamic range with which the system has to cope. The time scale of the variations depends on the velocity of the turbulent eddies transversal to the optical beam. In FSO from HAPs, this correlation time is on the order of milliseconds, and thus, typically much larger than the bit duration (picoseconds to nanoseconds). Hence, the optical power level of the received signal is constant over a large number of bits. Compared to the bit duration, the fading is "slow." Thus, system performance has to be characterized via an outage probability p_{BER}, which is the probability that the communication link cannot be closed [15].

Also, several measures to improve the communication quality during fading were already investigated.

1) Forward-Error Correction: Typical FEC chips in terrestrial systems need an input BER around 10^{-3} to achieve an output BER of better than 10^{-15} [15]. The International Telecommunication Union (ITU) standard G.975 uses a 16-way interleaved Reed–Solomon (RS)(255, 239) code with a 7% coding overhead that can correct error bursts of up to 1024 bits. At a data rate of $R = 10.7$ Gb/s, these 1024 correctable bits correspond to a duration of 95.7 ns, which is still very short compared to the microseconds to milliseconds time scale of power fluctuations caused by the atmosphere [15], [42]. Events during which more than 1024 consecutive bits are disturbed lead to a fading-induced outage. The outage probability describes the probability by which the actual BER is larger than a certain target value BER_t after the optical receive power P was multiplied by a factor a_{ch}. This factor a_{ch} can be interpreted as a "short-term" power loss that has to be compensated for, so that the BER is larger than BER_t only with a probability p_{BER}. Fig. 6 shows an example for the loss $10\log(a_{\mathrm{ch}})$ when using the RS(255,239) code within an OOK optically preamplified DD system as a function of increasing turbulence strength, i.e., with increasing scintillation index, and for various probability values p_{BER} [15]. At $\sigma_I^2 = 0$, no additional power is required to close the link. At increased turbulence, the link can only be closed with a certain probability. Some 5 dB of additional optical power have to be available, for example, at $\sigma_I^2 = 0.1$ to close a link with an outage probability of $p_{\mathrm{BER}} = 10^{-12}$. If these 5 dB are not available, the link fails. Fig. 6 illustrates that when using FEC in, e.g., an HAP–satellite communication scenario-–with system design parameters, as given in [15] and σ_I^2 typically smaller than 0.025-–error-free FSO

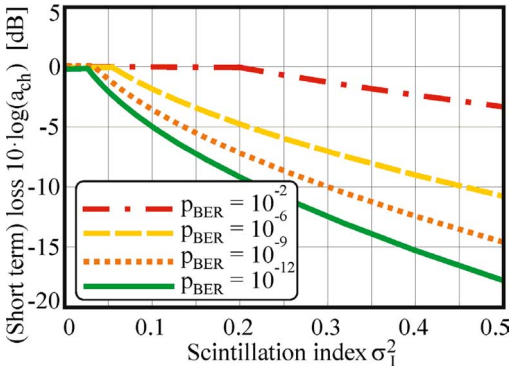

Fig. 6. Loss $a_{\rm ch}$ based on "short-term" BER versus scintillation index (as a function of the outage probability $p_{\rm BER}$), assumptions: HAP-to-GEO FSO link, $R = 10.7$ Gb/s, external modulation, optically preamplified receiver [15]; fade statistics with log normal PDF [5].

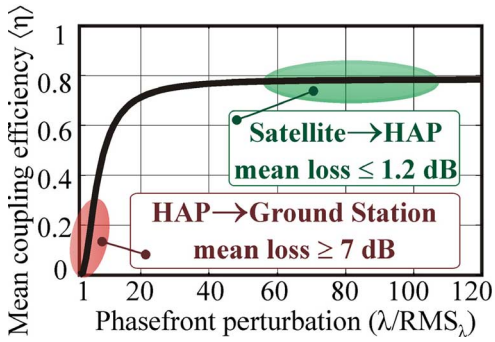

Fig. 7. Mean coupling efficiency into a standard single-mode fiber versus rms phase-front perturbation rms_λ given in fractions of the wavelength λ [46].

communication, i.e., a BER $= 10^{-9}$, is possible at $R = 10.7$ Gb/s with an outage probability better than 10^{-12}.

2) Wavelength Diversity: When dealing with long fade durations, very long FEC interleavers would have to be used to be effective [42]–[44]. Therefore, other methods were investigated to overcome deep fades. While the simplest way to reduce intensity-fading is the enlargement of the receive telescope diameter, such measures are usually not applicable onboard HAPs, where small telescope assemblies are required. One promising diversity concept makes use of the wavelength-dependent index of refraction of the atmosphere. For two or more wavelength channels of sufficient spectral distance, the received powers will show statistically independent behavior [43], and thus, a classical diversity receiver scheme (e.g., switched combining, equal-gain combining, or maximal-ratio combining) can be applied. Studies [43], [44] suggest that especially for HAP-to-HAP links, where the strongest turbulence is encountered in the middle of the path, and for ground–HAP scenarios, a very good decorrelation of signals can be achieved. For short paths, the beams pass essentially through the same parts of atmosphere and no wavelength diversity gain is to be expected.

3) Spatial Transmitter Diversity: Two or more telescopes transmitting the same signals are deployed. For sufficient spatial separation, which depends on the spatial coherence length [5], the two transmitter beams pass through statistically independent air masses [45]. If the signal fade statistics of the two beams become independent, the probability of deep fades is reduced. This method is only useable for ground-to-HAP links, as the scale size of the atmospheric turbulence at HAP platforms is too large to allow for a diversity effect.

D. Phase-front Distortions

When a laser beam propagates through the atmosphere, its phase front gets perturbed, which deteriorates the performance of coherent receivers and reduces the coupling efficiency into single-mode fibers [46]. If the turbulent eddies are relatively small compared to the beam diameter, e.g., in satellite-to-HAP or HAP-to-ground downlink scenarios, they lead to noticeable phase-front distortions within the receiving aperture. In uplink scenarios, where the turbulent eddies are right in front of the transmitter and comparatively large relative to the optical beam's cross section, phase-front disturbances are usually negligible within a small receiving aperture [5].

Fig. 7 gives the mean coupling efficiency as a function of the rms phase-front perturbation, rms_λ, expressed in fractions of the wavelength λ. For the calculations, we assumed $\lambda =$ 1550 nm and a standard telecommunication single-mode fiber with a core diameter of 10 μm, a core refractive index of 1.46, and a core/cladding refractive index difference of 0.3%. As expected, the characteristic shown in Fig. 7 is rather flat for small perturbations, but drops dramatically to very small values for large disturbances. For typical satellite-to-HAP communication links (i.e., altitude $h_{\rm HAP} > 17$ km, telescope diameter $D <$ 20 cm), the mean coupling loss is always less than 1.2 dB, while for communication links to a ground station, it significantly increases to values larger than 7 dB.

To counteract phase-front distortions, AO can be used. Conventional AO systems are based on the wavefront-conjugation principle, where phase-front aberrations are compensated by means of a deformable mirror [47]. These mirrors are characterized by the surface type, i.e., continuous or segmented, the actuation type, e.g., piezoelectric, electrostatic, or magnetic, the stroke, i.e., the maximum surface deformation, the number and arrangement of the actuators, and the bandwidth. The latter should be on the order of 10 kHz for quasi-geostationary HAPs to allow for real-time correction of atmospheric wavefront distortions. An optoelectronic feedback loop controls the mirror [48]. It comprises a wavefront sensor to measure the residual wavefront error. The Shack–Hartmann sensor, for example, consists of a lenslet array and a CCD detector placed in the back focal plane of the array. Each lenslet produces a spot on the detector. The displacement of the spot is proportional to the gradient of the wavefront across the lenslet. Alternatively, wavefront-sensorless AO systems, which directly use the power coupled into the fiber to correct phase distortions with an iterative method can be applied [49].

E. Weather Phenomena

Changing weather conditions result in atmospheric loss variations by several orders of magnitude. Even light clouds interrupt the link to ground stations, thus causing attenuation of several tens of decibels [14]. European studies on the availability statistics of optical HAP-to-ground links show single-link

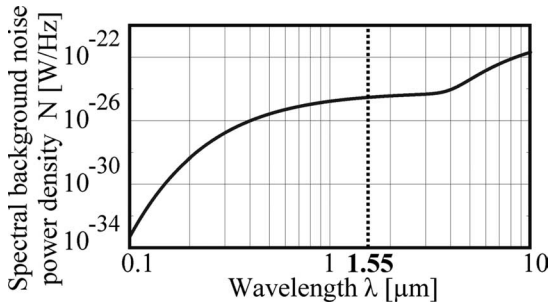

Fig. 8. Background noise power spectral density of the Earth received by a diffraction-limited telescope onboard an HAP.

availabilities ranging from <20% during winter in Northern Europe to over 70% during summer in Southern Europe [4], [25]. Using a ground-station diversity scheme, with ground stations at geographically separate locations, the availability increases with the number of available stations. The scheme requires an inter-HAP network to route the traffic toward the available ground links. Four stations over Southern Europe can achieve a 99% availability [25].

VI. Background Noise

In an FSO communication link, the receiver not only detects the signal from the transmitter, but also unwanted light from celestial bodies [50]. This may degrade system performance. The spectral radiance of electromagnetic radiation at wavelength λ from a self-emitting source at temperature T_{SE} is described by Planck's law of black body radiation

$$R(\lambda, T_{\mathrm{SE}}) = \frac{2hc^2}{\lambda^5} \frac{1}{\exp(hc/\lambda k T_{\mathrm{SE}}) - 1} \tag{7}$$

where h and k are Planck's and Boltzmann's constants, respectively, and c is the speed of light. The major source of background radiation is the Sun. When the receiver is at the HAP, sunlight is reflected from Earth and a certain amount of background radiance has to be expected from the sky also due to scattered sunlight.

By employing the definition of the spectral radiance, the power spectral density in watt per hertz accepted by the receiver's telescope originating from a radiating body is as follows:

$$N = A_{\mathrm{eff}} \frac{D^2 \pi \lambda^2}{4L^2 c} R(\lambda, T_{\mathrm{SE}}). \tag{8}$$

It depends on D, the receive telescope diameter, L, the distance between the receiver and the radiating body, and A_{eff}, the area of the radiating body, as seen from the receivers FOV at the distance L [31], [50]. Fig. 8 shows the power spectral density N caused by background radiation from Earth, i.e., for a ground station-to-HAP communication scenario, as a function of the wavelength λ for a diffraction-limited receive telescope with diameter $D = 0.135$ m. Both self-emission and reflected sunlight are taken into account, which is the reason why the curve shows two humps. At a communication wavelength of 1550 nm, N amounts to 2.89×10^{-25} W/Hz. For satellite-to-HAP scenarios, where background light results from the atmosphere due to scattering of incident radiation and because of emission by atmospheric particles as a result of absorption of incident radiation, the power spectral density is considerably less. This is shown in Table V, which gives example of background power spectral densities during daytime in clear sky conditions and during nighttime [31].

TABLE V
Background Power Spectral Density at 1550 nm Caused by Atmospheric Scattering

Atmospheric conditions	N [W/Hz]	Scenario
Day time, clear sky	1.54E-26	Satellite-to-ground
	8.87E-28	Satellite-to-HAP
Night time, clear sky	3.57E-33	Satellite-to-ground
	2.05E-34	Satellite-to-HAP

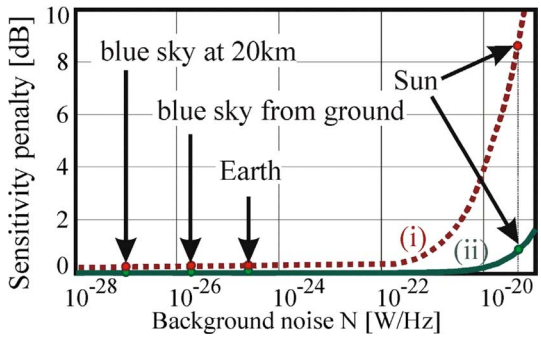

Fig. 9. Receiver sensitivity penalty (given relative to sensitivity without background noise) versus background noise power spectral density of (i) APD-based receiver and (ii) single-mode-coupled optically preamplified receiver. (Parameters: $\lambda = 1550$ nm, RZ intensity modulation, and BER $= 10^{-9}$.)

The influence of background radiation may be reduced by spectral, spatial, and polarization filtering.

1) Coherent Reception: Spectral filtering can be obtained in the IF section. Spatial filtering is inherent to the mixing process of the input radiation with the LO. If the LO operates in a single-transverse mode and in a single polarization only, a single spatial background mode in a single polarization will be detected.

2) DD, Low Data Rate, No Optical Preamplification: When optical filters as narrow as the signal spectrum are not available, e.g., when using the modulation formats discussed in Section III at data rates in the megabit-per-second range, effective spectral filtering cannot be obtained. Spatial filtering is governed by the instantaneous FOV of the receive telescope and the extension of the background source [50]. If the telescope is not diffraction-limited, the number of received background modes can be quite high.

3) DD, High Data Rate, Optical Preamplification: Optical filters with a bandwidth as narrow as 10 GHz, or even below when using pulse-shaping, are available today, e.g., in the form of fiber Bragg gratings in combination with optical circulators [12], [28]. Hence, spectral filtering can be very effective if Doppler frequency shifts are negligible or can be compensated. Spatial filtering is obtained by the coupling of the receive signal into a single-mode fiber, e.g., the pigtail of a preamplifying EDFA, which reduces the vulnerability to background light because only one spatial mode is detected.

Fig. 9 compares the receiver sensitivity penalty, given relative to the case where there is no background light at all, of an

APD-based receiver with a FOV of 90 μrad (dotted line) and a single-mode-coupled optically preamplified receiver (solid line) [31], [46]. In the case of blue sky as background source, only little degradation of receiver performance is found. Even when directly looking into the Sun, only an additional deterioration of 1.4 dB has to be expected in the case of a single-mode fiber-coupled receiver, clearly demonstrating the excellent spatial filter function of the fiber. According to [31], APD-based receivers suffer significantly more from background noise, because more than one spatial mode of the background light is received by the active area of the photodiode. When directly looking toward the Sun, the receiver performance will degrade by more than 8 dB.

VII. Studies on Optical Communications for HAPs

A. Satellite–HAP Communications

Several theoretical studies on satellite–HAP links have been published over the past years. Knapek *et al.* [25] investigated the achievable throughput of low Earth orbit (LEO) satellites to the ground. Several networking scenarios, including HAPs as relay stations, were shown. Data rates of 5.6 Gb/s were assumed based on the current laser communication terminal on TerraSAR-X [3]. A comparison with possible hybrid links that incorporate typical state-of-the-art microwave systems with 300 Mb/s was given, showing that optical links in combination with RF backup links can significantly increase the transfer volume per day. Based on global cloud statistics and stratospheric wind velocities, an optimal position for HAP relays was searched. While the link time for LEO satellite-to-HAP links increases at higher latitudes, the overall data transfer volume is almost constant because cloud coverage worsens near the poles. Additionally, stratospheric wind speeds are maximal around $\pm 60^\circ$ latitude, which complicates station keeping. Therefore, geographic latitudes around $\pm 30^\circ$ are most favorable. Giggenbach *et al.* [51] put emphasis on geometric visibility constraints between satellites, HAPs, and ground stations. Considerations were given to terminal architecture and the selection of optimum transmission technologies. Perlot *et al.* [33] worked on the properties of satellite–HAP communication channels. Atmospheric turbulence and link blockage by clouds were treated. Fidler [15] investigated the feasibility of optical communication links at $\lambda = 1550$ nm through the atmosphere between HAPs and geostationary satellites, for data rates up to 10.7 Gb/s and when applying FEC. The proposed communication system uses externally modulated return-to-zero (RZ) ON/OFF keying, an Erbium-doped optical booster amplifier with 10 W output power, and a single-mode fiber-coupled optically preamplified DD receiver. The investigated receiver shows a sensitivity that is only 1.6 dB above the quantum limit [46]. The optical link can be closed with an outage probability better than 10^{-12} at a BER of 10^{-9} (see cf., Fig. 6). Betti *et al.* addressed an HAP-GEO-HAP link [26] and an HAP–LEO scenario [17] using DPSK modulation, which offers up to 3 dB performance improvement compared to OOK. In 2006, Cazaubiel *et al.* [24] described the European Aeronautic Defence and Space Company (EADS) Astrium-coordinated development of an aircraft terminal in the project Liaison Optique Laser Aéroportée (LOLA) for communication between an aircraft and the geostationary orbit (GEO) satellite ARTEMIS. The communication of ARTEMIS with LEO satellites, the French SPOT-4 [18] and the Japanese OICETS [2], and downlinks to ESA's optical ground station on Tenerife [1] had already been demonstrated since 2001. The LOLA terminal was designed to cope with the increased difficulty of a moving aircraft. Data were planned to be transmitted at 848 nm and with 50 Mb/s to the satellite.

B. HAP-to-HAP Communications

In 2002, Giggenbach *et al.* [38] studied the concept of HAP interplatform links aiming at large-scale communication networks above the cloud layer. Important outcome of their work was that for moderate geographic latitudes, a maximum cloud height of only 13 km can be assumed. HAP-to-HAP optical paths above this altitude are not affected by cloud blockage. The 13-km cloud ceiling limits the maximum transmission distance, e.g., to $L = 600$ km for 20 km platform height. A theoretical analysis for HAP-to-HAP links at 20 km altitude was also conducted in [52], assuming a distance of 500 km, a communication wavelength of 1550 nm, intensity modulation, and a quadrature APD (QAPD) based receiver. The QAPD is used to implement both the PAT and the communication system with the help of only one photodetector. The system allows for a BER of 10^{-6} at a data rate of 384 Mb/s and a transmit power of 800 mW. Gangl *et al.* [53] investigated the development of aircraft communication terminals considering interaircraft and also aircraft-to-ground links. In 2006, first field trials of the terminals, working at 1550 nm, were performed on ground. The bidirectional communication links were tested over a distance of up to 2 km at a data rate of 2.5 Gb/s.

Several studies were conducted addressing networking aspects of optical HAP-to-HAP communication. Fortuna *et al.* [29] described optical backbone networks between HAPs. They investigate the physical constraints of dense wavelength-division-multiplexing optical connections and discuss issues of all-optical routing in the network. Adaptive routing yields better results than fixed or fixed alternate routing in terms of blocking probability and wavelength channel utilization. The required number of communication wavelengths is estimated with the aim of full interconnectivity without wavelength conversion. De Rango *et al.* [54] presented a quality-of-service aware routing algorithm based on ant colonies behavior, which aims at path-length minimization and load balancing on the HAP network. As outlined in Section V, the improvement of link availability from 20% up to 99% with the concept of ground-station diversity has also already been studied [4].

C. Ground–HAP Communications

In 2003, Jet Propulsion Laboratory (JPL) reported on the development of an optical terminal designed for the UAV Altair, which was planned to fly at 18 km altitude. The communication link was planned for 2.5 Gb/s, a link distance of 50 km, and a wavelength of 1550 nm [30]. The DLR performed a unidirectional optical downlink from a stratospheric balloon to a ground station within the EU project Capanina [14]. The terminal on the balloon was equipped with a communication transmitter for 1.25 Gb/s at 1550 nm. The PAT functionality was implemented

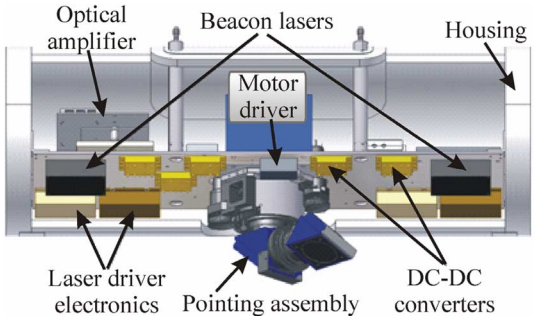

Fig. 10. Stratospheric flight terminal with the periscope-type coarse pointer.

Fig. 11. (Left) Photograph of the stratospheric balloon during launch preparations for CAPANINA. (Right) Near-infrared photograph of flight terminal below stratospheric balloon.

using an 810 nm beacon at the ground station and a 977 nm beacon at the balloon terminal. Communication could be demonstrated over 64 km at a BER of 3×10^{-7}. Fig. 10 shows a sketch of the flight terminal. Fig. 11 (left) depicts the preparations for the launch of the stratospheric balloon, and Fig. 11 (right) shows the payload below the balloon, as seen from the ground station's tracking camera. The balloon's GPS position was transmitted via an RF link to the ground station to enable initial link acquisition. As a follow-on, the DLR internal project Argos investigated the application of airborne real-time monitoring for applications, like disaster management or traffic observation. In this project, a second-generation optical terminal was built in 2007/2008 for the deployment on an aircraft. First unidirectional downlink tests of the terminal were performed in 2008 over a distance of up to 40 km [55]. The system featured an acquisition method without additional beacons. The laser beams at 1550 nm from the flight terminal 1590 nm from the ground station, respectively, were used at the same time for PAT and communications. The PAT systems of both terminals used InGaAs cameras operating at 1550/1590 nm.

VIII. Summary and Conclusion

Optical free-space communication for HAPs benefits from technologies, which were initially developed for terrestrial fiber-based and satellite laser communication. Main differences arise due to the influence of the atmosphere on the laser beam, thus leading to loss and time-variant power fading, the requirement for very agile PAT systems due to the relatively unstable platforms, which are mostly still under development, and different requirements on maximum payload weight, power consumption, or flight qualification compared to outer space systems. Trials showed FSO communication at 1.25 Gb/s for downlinks to the ground, while experimental and theoretical studies predict the feasibility of HAP-to-HAP and HAP–satellite links with up to 10 Gb/s based on current technology.

Acknowledgment

The authors would like to thank J. M. Perdigues-Armengol (ESA), K. Kudielka, and T. Dreischer (RUAG Space AG) for valuable discussions.

References

[1] Z. Sodnik, B. Furch, and H. Lutz, "Free-space laser communication activities in Europe: SILEX and beyond," in *Proc. IEEE Lasers Electro-Opt. Soc.*, 2006, pp. 78–79.

[2] T. Jono, Y. Takayama, K. Shiratama, I. Mase, B. Demelenne, Z. Sodnik, A. Bird, M. Toyoshima, H. Kunimori, D. Giggenbach, N. Perlot, M. Knapek, and K. Arai, "Overview of the inter-orbit and the orbit-to-ground laser communication demonstration by OICETS," *SPIE*, vol. 6457, pp. 645702-1–645702-10, 2007.

[3] R. Lange, F. Heine, H. Kämpfner, and R. Meyer, "High data rate optical inter-satellite links," presented at the Eur. Conf. Opt. Commun. (ECOC 2009), Vienna, Austria, Paper 10.6.1.

[4] F. Moll and M. Knapek, "Wavelength selection criteria and link availability due to cloud coverage statistics and attenuation affecting satellite, aerial, and downlink scenarios," *SPIE Free-Space Laser Commun. VII*, vol. 6709, pp. 670916-1–670916-12, 2007.

[5] L. C. Andrews and R. L. Phillips, *Laser Beam Propagation through Random Media*, 2nd ed. Bellingham, WA: SPIE, 2005.

[6] COST297. (2010, Jan.). HAPCOS—High Altitude Platforms for Communications and Other Services [Online]. Available: http://www.hapcos.org

[7] G. Avdikos, G. Papadakis, and N. Dimitriou, "Overview of the application of high altitude platform (HAP) systems in future telecommunication networks," in *Proc. 10th Signal Process. Space Commun.*, 2008, pp. 1–6.

[8] G. Baister and P. V. Gatenby, "Pointing, acquisition, and tracking for optical space communications," *IEEE Electron. Commun. Eng. J.*, vol. 6, no. 6, pp. 271–280, Dec. 1994.

[9] J. Horwath, N. Perlot, M. Knapek, and F. Moll, "Experimental verification of optical backhaul links for high-altitude platform networks: Atmospheric turbulence and downlink availability," *Int. J. Satellite Commun. Netw.*, vol. 25, no. 5, pp. 501–528, 2007.

[10] T. C. Tozer and D. Grace, "High-altitude platforms for wireless communications," *Electron. Commun. Eng. J.*, vol. 13, no. 3, pp. 127–137, 2001.

[11] R. Miura and M. Suzuki, "Preliminary flight test program on telecom and broadcasting using high altitude platform stations," *Wireless Pers. Commun.*, vol. 24, pp. 341–361, 2003.

[12] H. Hemmati, *Near-Earth Laser Communications*. Boca Raton, FL: CRC Press, 2009.

[13] M. Toyoshima, W. R. Leeb, H. Kunimori, and T. Takano, "Comparison of microwave and lightwave communication systems in space applications," *Opt. Eng.*, vol. 46, no. 1, pp. 015003-1–015003-7, 2007.

[14] J. Horwath, M. Knapek, B. Epple, M. Brechtelsbauer, and B. Wilkerson, "Broadband backhaul communication for stratospheric platforms: The stratospheric optical payload experiment (STROPEX)," *Proc. SPIE*, vol. 6304, pp. 63041N-1–63041N-12, 2006.

[15] F. Fidler, "Optical backhaul links between HAPs and satellites in the multi-Gigabit regime," in *Proc. Globecom Workshop Collection*, 2008, pp. 1–5.

[16] B. J. Klein and J. J. Degnan, "Optical antenna gain. 1: Transmitting antennas," *Appl. Opt.*, vol. 13, no. 9, pp. 2134–2141, 1974.

[17] M. Antonini, S. Betti, V. Carrozzo, E. Duca, and M. Ruggieri, "Feasibility analysis of a HAP-LEO optical link for data relay purposes," presented at the Aerosp. Conf., Big Sky, MT, 2006.

[18] G. Planche and V. Chorvalli, "SILEX in-orbit performances," in *Proc. 5th Int. Conf. Space Opt.*, 2004, pp. 403–410.

[19] RUAG Space AG. (2009, Oct.). Optel AP [Online]. Available: http://www.ruag.com

[20] B. Smutny, R. Lange, G. Mühlnikel, and F. Heine, "Coherent laser communications terminals for LEO-GEO data links," presented at the 14th Coherent Laser Radar Conf. (CLRC), Snowmass, CO, 2007.

[21] W. R. Leeb, "Heterodyne and homodyne detection in optical space communications," in *Proc. Opt. Space Commun.*, 1989, pp. 216–223.

[22] A. Leven, "Coherent receivers: Principles and real-time implementation," in *Proc. Eur. Conf. Opt. Commun. (ECOC 2009)*, pp. 1–27, Paper 6.6.3.
[23] P. J. Winzer and R. J. Essiambre, "Advanced optical modulation formats," *Proc. IEEE*, vol. 94, no. 5, pp. 952–985, May 2006.
[24] V. Cazaubiel, G. Planche, V. Chorvalli, L. Le Hors, B. Roy, E. Giraud, L. Vaillon, F. Carré, and E. Decourbey, "LOLA: A 40.000 km optical link between an aircraft and a geostationary satellite," presented at the 6th Int. Conf. Space Opt., Noordwijk, The Netherlands, 2006.
[25] M. Knapek, J. Horwath, F. Moll, B. Epple, N. Courville, H. Bischl, and D. Giggenbach, "Optical high-capacity satellite downlinks via high altitude platform relays," in *Proc. SPIE Free-Space Laser Commun. VII*, vol. 6709, pp. 6709E-1–6709E-12, 2007.
[26] S. Betti, E. Duca, and I. Toselli, "HAP-GEO optical links: Performance analysis under weak turbulence conditions," in *Proc. Symp. Commun. Syst., Netw. Digit. Signal Process.*, 2008, pp. 77–81.
[27] F. Fidler, J. Grosinger, and W. R. Leeb, "Sensitivity of balanced receivers for polarization shift keying in free-space optical communications," *Eur. Conf. Opt. Commun. (ECOC 2009)*, pp. 1–2, Paper 9.6.2.
[28] D. O. Caplan, "Laser communication transmitter and receiver design," in *Free-Space Laser Communications: Principles and Advances*, A. Majumdar and J. C. Ricklin, Eds. New York: Springer-Verlag, 2007, pp. 109–271.
[29] C. Fortuna, A. Vilhar, J. Horwath, and M. Mohorcic, "Wavelength requirements in optical transport networks based on high altitude platforms," in *Proc. Symp. Commun. Syst., Netw. Digit. Signal Process.*, 2008, pp. 87–91.
[30] A. Biswas, "Airborne optical communications demonstrator design and pre-flight test results," *Proc. SPIE Free-Space Laser Commun. Technol. XVII*, vol. 5712, pp. 205–216, 2005.
[31] F. Fidler. (2007, Sep.). Optical Communications from High Altitude Platforms (Dissertation), Inst. Commun. Radio-Frequency Eng., Vienna Univ. Technol., Vienna, Austria. [Online]. Available: http://publik.tuwien.ac.at/files/PubDat_112010.pdf
[32] N. W. Spellmeyer, D. O. Caplan, B. S. Robinson, D. Sandberg, M. L. Stevens, M. M. Willis, D. V. Gapontsev, N. S. Platonov, and A. Yusim, "A high-efficiency Ytterbium-doped fiber amplifier designed for interplanetary laser communications," in *Proc. Opt. Fiber Commun. Conf. (OFC 2007)*, pp. 1–3, Paper OMF2.
[33] N. Perlot, E. Duca, J. Horwath, D. Giggenbach, and E. Leitgeb, "System requirements for optical HAP-satellite links," in *Proc. Symp. Commun. Syst., Netw. Digit. Signal Process.*, 2008, pp. 72–76.
[34] J. M. Perdigues-Armengol, "European space agency," presented at the Pers. Commun., Noordwijk, The Netherlands, Oct. 2009.
[35] Y. Fujiwara, M. Mokuno, T. Jono, T. Yamawaki, K. Arai, M. Toyoshima, H. Kunimori, Z. Sodnik, A. Bird, and B. Demelenne, "Optical inter-orbit communications engineering test satellite (OICETS)," *Acta Astronautica*, vol. 61, pp. 163–175, 2007.
[36] A. Harris, J. J. Sluss, H. H. Refai, and P. G. LoPresti, "Alignment and tracking of a free-space optical communication link to a UAV," in *Proc. 24th Digit. Avionics Syst. Conf.*, 2005, pp. 1.C.2-1–1.C.2-9.
[37] W. K. Pratt, *Laser Communication Systems*, 1st ed. New York: Wiley, 1969.
[38] D. Giggenbach, R. Purvinskis, M. Werner, and M. Holzbock, "Stratospheric optical interplatform links for high altitude platforms," presented at the 20th AIAA Int. Commun. Satellite Syst. Conf. Exhib., Montreal, QB, Canada, 2002.
[39] B. Mayer, S. Shabdanov, and D. Giggenbach, "Atmospheric absorption database," German Aerosp. Center (DLR), DLR-Oberpfaffenhofen, Tech. Rep. DLR-IPA and DLR-KN-DN-OCG, 2002.
[40] H. Kogelnik and T. Li, "Laser beams and resonators," *Proc. IEEE*, vol. 54, no. 10, pp. 1312–1329, Oct. 1966.
[41] P. D. Stroud, "Statistics of intermediate duration averages of atmospheric scintillation," *Opt. Eng.*, vol. 35, no. 2, pp. 543–548, 1996.
[42] H. Henniger, F. David, D. Giggenbach, and C. Rapp, "Evaluation of FEC for the atmospheric optical IM/DD channel," *Proc. SPIE*, vol. 4975, pp. 1–11, 2003.
[43] D. Giggenbach, B. L. Wilkerson, H. Henniger, and N. Perlot, "Wavelength-diversity transmission for fading mitigation in the atmospheric optical communication channel," *Proc. SPIE*, vol. 6304, pp. 63041H-1–63041H-12, 2006.
[44] A. Harris, J. J. Sluss, Jr., H. H. Refai, and P. G. LoPresti, "Free-space optical wavelength diversity scheme for fog mitigation in a ground-to-unmanned-aerial-vehicle communications link," *SPIE Opt. Eng.*, vol. 45, no. 8, pp. 086001-1–086001-12, 2006.
[45] D. Giggenbach, F. David, R. Landrock, K. Pribil, E. Fischer, R. Buschner, and D. Blaschke, "Measurements at a 61-km near-ground optical transmission channel," *Proc. SPIE*, vol. 4635, pp. 162–170, 2002.
[46] F. Fidler and O. Wallner, "Application of single-mode fiber-coupled receivers in optical satellite to high altitude platform communications," *EURASIP J. Wireless Commun. Netw.*, vol. 2008, pp. 864031-1–864031-7, 2008, Article ID 864031.
[47] N. Devaney, E. Dalimier, T. Farrell, D. Coburn, R. Mackey, D. Mackey, F. Laurent, E. Daly, and Ch. Dainty, "Correction of ocular and atmospheric wavefronts: A comparison of the performance of various deformable mirrors," *Appl. Opt.*, vol. 47, no. 35, pp. 6550–6562, 2008.
[48] R. Mackey, D. Thornton, and C. Dainty, "Towards a high speed adaptive optics system for strong turbulence compensation," *Proc. SPIE*, vol. 5981, pp. 183–187, 2005.
[49] T. Weyrauch, M. A. Vorontsov, J. W. Gowens, II, and T. G. Bifano, "Fiber coupling with adaptive optics for free-space optical communication," *Proc. SPIE*, vol. 4489, pp. 177–184, 2002.
[50] W. R. Leeb, "Degradation of signal to noise ratio in optical free-space data links due to background illumination," *Appl. Opt.*, vol. 28, pp. 3443–3449, 1989.
[51] D. Giggenbach, B. Epple, J. Horwath, and F. Moll, "Optical satellite downlinks to optical ground stations and high altitude platforms," in *Proc. IST Mobile Wireless Commun. Summit*, 2007, pp. 1–4.
[52] E. Katimertzoglou, D. Vouyioukas, P. Veltsistas, and P. Constantinou, "Optical interplatform link scenarios for 20 km altitude," in *Proc. 16th IST Mobile Wireless Commun. Summit*, 2007, pp. 1–5.
[53] M. E. Gangl, D. S. Fisher, J. A. Cunningham, D. Foulke, T. M. Fletcher, D. Grinch, D. Jeri, D. Hopf, T. Goode, and D. Baber, "Fabrication and testing of laser communication terminals for aircraft," *Proc. SPIE*, vol. 6243, pp. 624304-1–624304-11, 2006.
[54] F. De Rango, M. Tropea, A. Provato, A. F. Santamaria, and S. Marano, "Multiple metrics aware ant routing over HAP mesh networks," in *Proc. Can. Conf. Electr. Comput. Eng. (CCECE 2008)*, pp. 1675–1678.
[55] J. Horwath and C. Fuchs, "Aircraft to ground unidirectional laser-comm. terminal for high resolution sensors," *Proc. SPIE*, vol. 7199, pp. 7199-1–7199-8, 2009.

Franz Fidler received the Dipl.-Ing. (M.Sc.) and Dr. (Ph.D.) degrees in electrical/communications engineering from the Vienna University of Technology, Vienna, Austria, in 2004 and 2007, respectively.

From 2008 to 2009, he was a Postdoctoral Research Fellow at Columbia University, New York, and Bell Laboratories, Murray Hill, NJ, where he was involved in investigating cross-layer information exchange in optical networks. He is currently with the Institute of Communications and Radio-Frequency Engineering, Vienna University of Technology. His academic work, mostly supported by the European Space Agency, has been focused on high-speed optical free-space communications. During several research visits at Bell Laboratories, Holmdel, he was involved in investigating performance-enhancement measures in wavelength-division multiplexing networks, which involved the use of vertical-cavity surface-emitting lasers, advanced modulation formats, and high-speed field-programmable gate arrays.

Markus Knapek received the M.Sc. degree in electrical engineering from the City University of New York, New York, in 1996, and the Dipl.-Ing. degree from the University of Technology Munich, Munich, Germany, in 1999.

Since 2003, he has been a Scientist in the group for optical free-space communications at the German Aerospace Center (DLR), Oberpfaffenhofen, where he was responsible for the development of DLR's Optical Ground Station, which included the design of the pointing, acquisition, and tracking system and the atmospheric measurement instruments. As a Technical Project Leader, he has led several measurement campaigns (Tenerife, Calar Alto, Oberpfaffenhofen). Since 2007, he has been involved in the research in the introduction of the new field of adaptive optics for satellite communications in the group and supervises the work from the scientific side.

Joachim Horwath received the Dipl.-Ing. (M.Sc.) degree in electrical engineering from the University of Graz, Graz, Austria, in 2002.

Since 2002, he has been a Staff Member at the Institute of Communications and Navigation, German Aerospace Centre (DLR), Wessling, Germany. He was involved in several research projects focusing on free-space optical communication for high-altitude platforms, satellites, and avionic applications and is responsible for the development of optical terminals. His current research interests include atmospheric turbulence effects on coherent and incoherent optical communication links and numerical simulation of turbulent wave propagation.

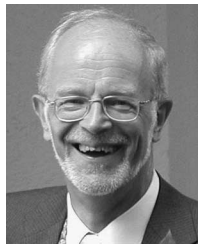

Walter R. Leeb received the M.Sc. and Dr.Sc. technical degrees in electrical engineering as well as the Habilitation degree in optical communications from the Vienna University of Technology, Vienna, Austria.

In the 1970s, he was at the NASA Goddard Space Flight Center, Greenbelt, MD for two postdoctoral years. He is currently at the Institute of Communications and Radio-Frequency Engineering, Vienna University of Technology, where he was a Research Assistant, a Lecturer, and then, a Professor from 1982 to 2007. His research interests include research and development works in the area of optoelectronic devices and laser communication systems (coherent reception, intersatellite laser links, optical phased-array antennas, wavelength-division-multiplexing fiber systems), stellar interferometry, and quantum communications using entangled photons.